The Starlink Robot: A Platform and Dataset for Mobile Satellite Communication

Abstract

The integration of satellite communication into mobile devices represents a paradigm shift in connectivity, yet the performance characteristics under motion and environmental occlusion remain poorly understood. We present the Starlink Robot, the first mobile robotic platform equipped with Starlink satellite internet, comprehensive sensor suite including upward-facing camera, LiDAR, and IMU, designed to systematically study satellite communication performance during movement. Our multi-modal dataset captures synchronized communication metrics, motion dynamics, sky visibility, and 3D environmental context across diverse scenarios including steady-state motion, variable speeds, and different occlusion conditions. This platform and dataset enable researchers to develop motion-aware communication protocols, predict connectivity disruptions, and optimize satellite communication for emerging mobile applications from smartphones to autonomous vehicles. In this work, we use LEOViz for real-time data collection and visualization. The project is available at https://starlinkrobot.github.io.

Keywords

Satellite Communication, Mobile Systems, Robot, Starlink

1 Introduction

The landscape of global connectivity is undergoing a fundamental transformation. SpaceX's Starlink constellation has deployed over 5,000 satellites, delivering high-speed internet to previously unreachable locations [25]. This success has catalyzed a broader revolution: major technology companies including Apple, Samsung, and Google are racing to integrate satellite communication capabilities directly into consumer smartphones, with Apple's Emergency SOS already saving lives in remote locations and Google partnering with Skylo for Android satellite messaging [5, 16].

Yet this promise faces a critical challenge. Current satellite internet deployments predominantly serve stationary users – homes, businesses, and fixed installations [6]. The Starlink Mini's recent introduction has made portable satellite internet more accessible [25], but fundamental questions remain unanswered. How does motion affect satellite link quality? What happens when agricultural drones monitor vast farmlands beyond cellular coverage, or when emergency responders navigate disaster zones where terrestrial infrastructure has failed [4, 22]? These questions become urgent for applications where LTE simply cannot reach: maritime vessels tracking cargo across oceans, wildlife researchers following migrations in remote habitats, and autonomous vehicles traversing rural areas where cellular towers are economically unfeasible.

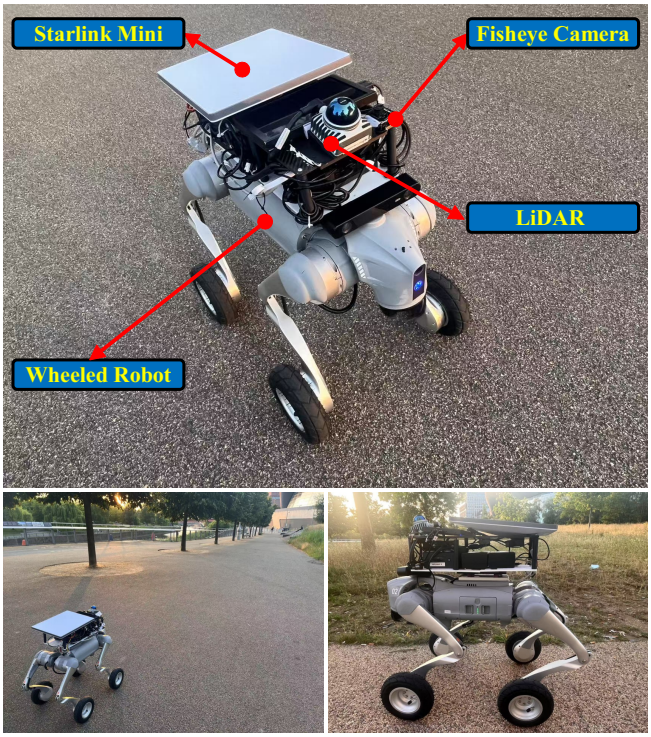

Figure 1. The Starlink Robot platform integrating a Unitree GO2 wheeled robot with Starlink Mini terminal, upward-facing fisheye camera, and Livox Mid-360 LiDAR for comprehensive mobile satellite communication research

The challenge extends beyond simple mobility. Satellite communication operates under fundamentally different constraints than terrestrial networks [4, 6, 8, 22]. A moving device must maintain connection with satellites traveling at 7.5 km/s while simultaneously dealing with local motion and environmental occlusions [4]. Trees, buildings, and even the device's own orientation can disrupt the delicate link between Earth and space [4, 22]. Unlike terrestrial networks where signal paths remain relatively stable, satellite links must contend with both terrestrial motion and satellites racing overhead at 27,000 km/h, creating a uniquely dynamic communication environment [4, 6, 8, 22]. Understanding these dynamics requires more than theoretical models – it demands real-world data collected under controlled yet realistic conditions [4, 6].

To address this gap, we developed the Starlink Robot shown in Figure 1, a purpose-built **platform** that brings together mobile robotics and satellite communication. Our approach transforms a Unitree GO2 wheeled robot into a mobile laboratory, equipped with Starlink Mini for connectivity and a suite of sensors to capture the complete context of communication performance. The upward-facing fisheye camera observes sky visibility, the Livox Mid-360 LiDAR

maps the surrounding environment, and integrated IMUs track every movement. This comprehensive sensing enables us to correlate communication metrics with physical conditions, revealing how motion and occlusion influence satellite connectivity.

Our contribution extends beyond the platform itself. We present a **multi-modal dataset** that synchronizes Starlink performance metrics – including latency, upload and download throughput, and signal quality indicators – with high-frequency motion data and environmental observations. Satellite tracking data is collected using LEOViz [3, 30], which provides real-time visualization of satellite positions and connection status. This dataset captures diverse scenarios from steady locomotion to variable speeds, from open sky to heavily occluded urban environments. By releasing both our platform design and collected data, we provide the research community with tools to develop the next generation of mobile satellite communication systems. Our initial dataset contains 7 hours of synchronized multi-modal data collected across diverse urban environments in London, with ongoing data collection expanding the dataset. The current release includes over 25K RTT measurements, 630k LiDAR frames, and 378k fisheye images, covering open areas, tree-covered paths, and urban environments at varying movement speeds.

2 Related Works

The rapid deployment of LEO satellite constellations has sparked significant research interest in characterizing their performance. The Starlink academic community, particularly through the University of Victoria's PanLab, has produced comprehensive studies of Starlink's several static performance characteristics [3, 7, 9, 11, 14, 15, 17, 18, 20, 23, 24, 26–29, 31, 32]. Among these, LEOViz [3, 30] provides real-time visualization and tracking of Starlink satellites, displaying satellite positions, elevation angles, and connection status. In our work, we utilize LEOViz as our data collection and visualization tool, running it alongside our robotic platform to record satellite tracking information during mobile experiments. The satellite data captured by LEOViz enables us to analyze satellite communication performance during movement. Kassem et al. analyzed throughput variations across geographic locations, revealing how latitude affects connection quality due to satellite density differences [12]. Muhammad et al. investigated weather impacts, demonstrating that rain fade affects Starlink less severely than traditional geostationary satellites due to shorter signal paths [21]. These foundational studies establish baseline performance metrics but explicitly acknowledge the limitation of stationary measurements.

Recent work has begun exploring mobility scenarios, though primarily in constrained settings. Laniewski et al. conducted preliminary tests with Starlink terminals in vehicles, reporting increased latency variance during highway driving [13]. However, their study lacked synchronized motion data and environmental context, making it difficult to isolate causative factors, and the dataset is not open-sourced. SpaceX Maritime [2] deployments documented by SpaceX show promising performance on ships, but the relatively stable motion and unobstructed ocean views present a best-case scenario that doesn't translate to terrestrial mobile applications. The fundamental challenge remains: no existing work provides the fine-grained, multi-modal data necessary to understand how specific motion patterns and environmental conditions affect satellite communication.

The robotics community has long recognized the value of mobile platforms for wireless communication research. The CRAWDAD repository [1] contains numerous datasets from robot-mounted WiFi experiments, demonstrating how controlled mobility can reveal network behavior patterns invisible in static deployments. More recently, researchers have employed drones to map 5G coverage, taking advantage of three-dimensional mobility to characterize cellular networks [19]. Yet these efforts remain confined to terrestrial communication systems [10]. The unique challenges of satellite communication – including the need for precise sky visibility, the impact of antenna orientation, and the effects of Doppler shift from dual mobility – require purpose-built platforms and measurement methodologies. Our work bridges this gap by adapting mobile robotics techniques specifically for satellite communication research, creating a reproducible platform that others can build upon.

Overall, our work proposes the first dedicated platform for *mobile satellite communication* research, providing the tools and data necessary to understand this emerging communication paradigm.

3 System Design

The Starlink Robot platform integrates three core subsystems to enable comprehensive mobile satellite communication research. As illustrated in Figure 2, the Mobile Platform subsystem combines the Unitree GO2 robot base with the Starlink Mini terminal, providing controlled mobility with precise velocity and position tracking. The Sensor Suite subsystem synchronizes multiple data streams: the Livox Mid-360 LiDAR captures 3D environmental geometry, the upward fisheye camera monitors sky visibility for obstruction detection, while IMU and GPS units track motion dynamics and global positioning. The Data Processing subsystem handles real-time synchronization of these heterogeneous data sources, logging both raw sensor data and processed metrics for offline analysis. This architecture enables researchers to correlate communication performance with environmental and motion contexts at millisecond precision.

3.1 Hardware Architecture

The hardware platform, shown in Figure 1, integrates mobility, communication, and sensing capabilities through a set of integrated components:

Mobile Base: The Unitree Go2 wheeled version provides the foundation with a 15 kg payload capacity and differential drive system. The wheeled configuration provides smooth,

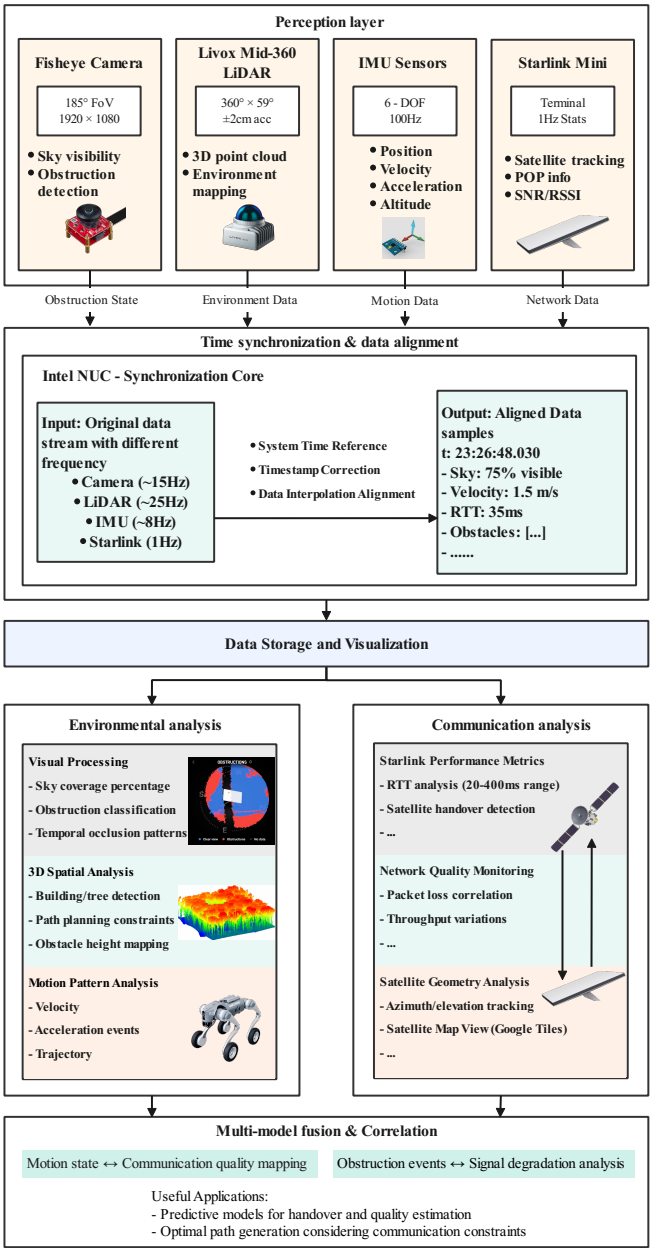

Figure 2. System architecture of the Starlink Robot platform showing multi-modal sensor integration, data synchronization pipeline, and analysis framework for correlating communication performance with environmental and motion context.

continuous movement that helps isolate communication variations from motion artifacts. The platform supports precise velocity control from 0.1 m/s to 2.0 m/s, covering typical pedestrian movement speeds.

Communication System: The Starlink Mini terminal is mounted on a 3D-printed support structure that replaces the earlier aluminum frame. The mount maintains a stable upward orientation and reduces vibration transmission from the base. The terminal connects to the onboard Intel NUC via Ethernet and receives power through a DC–DC converter that steps down the robot's 24 V supply to Starlink's 12 V input. In LEOViz, the Starlink gRPC interface is accessed through a local Python client for periodic telemetry queries.

Sensing Configuration: The sensing suite captures the environmental and motion context required for link analysis. It includes a Livox Mid-360 LiDAR (360° field of view at 25 Hz, 0.05 m range accuracy) and an upward-facing fisheye camera (185° FoV at 15 Hz) for sky-visibility monitoring. No dedicated IMU or GPS module is installed. Motion and localization data are instead obtained from the robot's internal SLAM estimator and the localization output of the built-in Starlink terminal.

Computing Platform: An Intel NUC running Ubuntu 18.04 with ROS Noetic serves as the central node, handling sensor synchronization, data logging, and real-time processing. All incoming data—including Starlink telemetry, SLAM motion traces, LiDAR frames, and camera images—are timestamped using the NUC's system clock as a unified time source, providing sub-millisecond alignment across modalities.

Power Consumption: During normal operation, the platform draws approximately 60–110 W for the mobile base (low to moderate speeds) and 20–40 W for the Starlink Mini terminal (about 15 W when idle). In field experiments, the system operated continuously and stably for about two hours per deployment without performance degradation.

3.2 Software Architecture

Mobile satellite communication research demands precise temporal alignment across diverse data streams to establish causal relationships between motion, environment, and performance. A position change of just one meter or an obstruction lasting mere seconds can dramatically impact satellite connectivity. Our ROS-based framework therefore treats time synchronization as a fundamental design principle. Each sensor node implements hardware triggering where available (LiDAR, camera) and kernel-level timestamping for software-triggered sensors (network metrics). A dedicated synchronization node correlates these timestamps against GPS time when available, achieving sub-millisecond alignment accuracy essential for correlating transient communication events with their physical causes.

The Starlink data collection presents unique challenges as the terminal doesn't expose a direct API. We employ a multi-layered approach: for satellite tracking and constellation data, we use LEOViz [3, 30], which handles the parsing of Starlink's gRPC status interface and provides 1Hz updates on satellite positions, azimuth/elevation angles, signal quality, and connection status. LEOViz visualizes this data in real-time and we record its output during our experiments.

The diverse sensors generate data at different rates that must be efficiently stored and synchronized. During experiments, the ROS framework saves LiDAR point clouds, camera images, and IMU measurements directly to bag files on the onboard computer's SSD. Network measurements from the Starlink terminal and our active probing tools are logged separately as CSV files with timestamps. After each session,

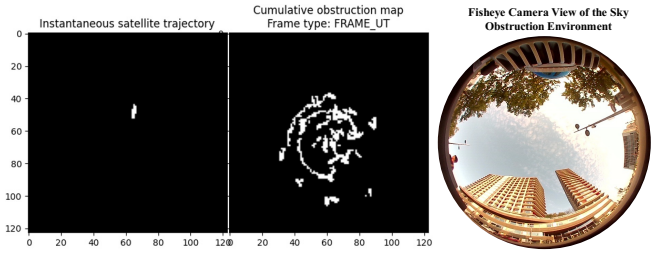

Figure 3. Starlink terminal's obstruction detection output (left) that is visualized by LEOViz [3, 30], and Dual-view obstruction analysis showing fisheye camera sky visibility (right), demonstrating real-time obstruction mapping capabilities.

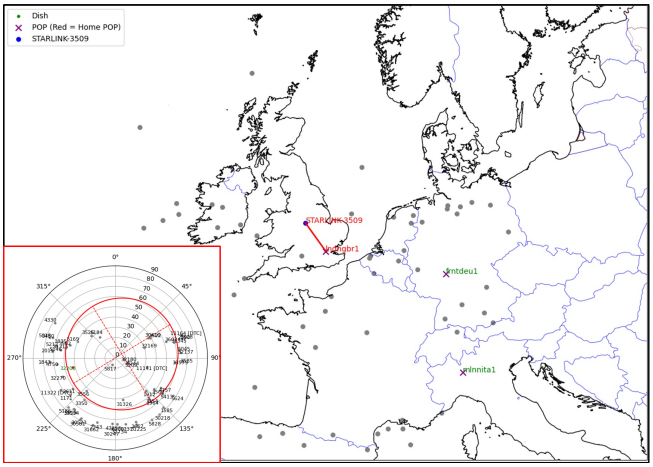

Figure 4. Satellite constellation visualization using LEOViz [3, 30], displaying active Starlink satellites' positions, elevation angles, and connection status relative to the robot's location during data collection.

we process these multiple data sources: our synchronization software reads the timestamps from each file, aligns them using the GPS clock as reference, and combines everything into a single HDF5 file. This unified format allows researchers to access all sensor data and communication metrics with consistent timestamps without dealing with multiple file formats.

4 Dataset Description

Our dataset represents 7 hours of synchronized multi-modal sensor data from the Starlink Robot platform, comprising approximately 120GB collected across diverse environmental categories in London: open spaces (40%), tree-covered areas (35%), and urban environments (25%). With 98.5% data completeness and sub-millisecond synchronization accuracy, this dataset provides the foundation for developing robust mobile satellite communication systems.

Obstruction Detection Data. As shown in Figure 3, we provide dual obstruction detection: fisheye camera images (1920×1080, 15Hz, 185-degree FOV) for sky visibility analysis, and Starlink terminal's internal obstruction detection output. Both streams are time-synchronized for comparison between visual obstruction and the terminal's algorithms.

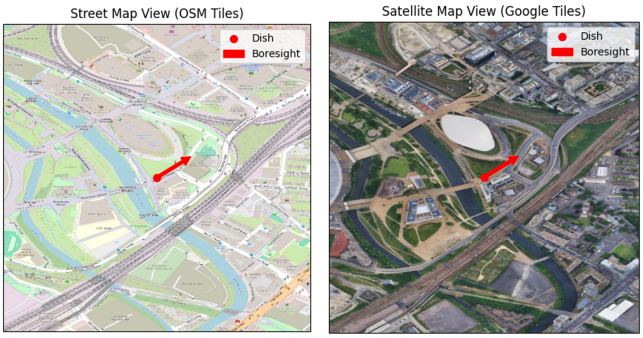

Figure 5. Google map view of the localization utilized LEOViz [3, 30].

Figure 6. LiDAR-based 3D point cloud visualization capturing environmental geometry around the robot, enabling precise obstruction detection.

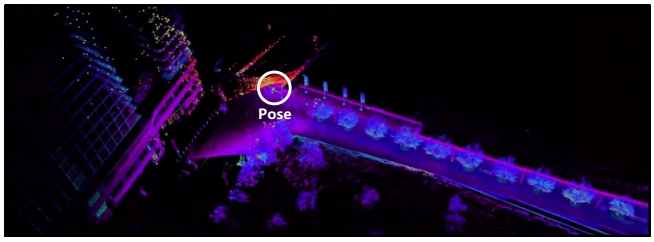

Figure 7. Robot pose and motion data indicating position, velocity, orientation, and trajectory information synchronized with communication performance metrics

Satellite Tracking Information. Figure 4 illustrates real-time satellite tracking data collected at 1Hz. For each visible satellite, we record azimuth, elevation, signal strength, and connection status, enabling analysis of handover patterns and satellite selection behavior during mobile operation.

Location and Path Data. GPS positioning at 1Hz provides global coordinates of the robot's trajectory (Figure 5). Our experimental paths cover diverse urban environments with varying obstruction characteristics, supplemented by wheel odometry at 8Hz for improved position accuracy.

3D Environmental Mapping. The Livox Mid-360 LiDAR captures 360-degree point clouds at 25Hz with 0.05m accuracy up to 40 meters (Figure 6), enabling 3D reconstruction and correlation with communication performance.

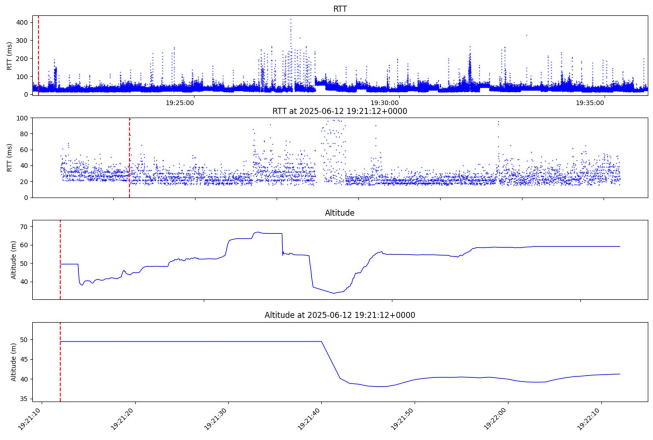

Figure 8. Multi-metric Starlink communication performance indicating RTT variations and altitude profiles during mobile operation.

Robot Motion and Pose Data. Figure 7 presents comprehensive motion data from IMU (8Hz) and wheel encoders, providing complete 6-DOF pose estimation including position, orientation, velocity, and acceleration to capture vibrations, turns, and speed variations.

Communication Performance Metrics. The core of our dataset is the Starlink communication measurements shown in Figure 8. We collect with LEOViz: (1) Terminal-reported statistics at 1 Hz including downlink/uplink throughput, RTT, SNR, and obstruction state; (2) Active network measurements with ICMP probes at 10 Hz to multiple servers; (3) TCP/UDP throughput tests every 30 seconds. All communication data is timestamped and synchronized with sensor data.

Data Format and Organization. The dataset follows a unified structure designed for easy parsing and synchronization. Raw sensor data are stored as ROS bag files, which contain LiDAR point clouds, fisheye camera images, IMU readings, and GPS information. Processed communication metrics and satellite tracking logs are exported as CSV files, while all synchronized multi-modal data are aggregated into HDF5 format for efficient analysis. Comprehensive documentation describing the dataset directory hierarchy, file naming conventions, and data schema (ROS bags, CSVs, and HDF5) is available on the companion site of https://starlinkrobot.github.io. The site also provides well-commented sample scripts for parsing, aligning, and visualizing the data, demonstrating how to reproduce major figures in the paper and extend the dataset for new experiments.

5 Preliminary Findings

To demonstrate our platform's utility, we present two case studies examining critical factors in mobile satellite communication. These analyses, conducted in the London Olympic Sports Center area, reveal how movement velocity and environmental transitions affect Starlink performance.

5.1 Impact of Movement Velocity

Experimental Setup: We conducted controlled velocity experiments along a 2km loop through open campus areas,

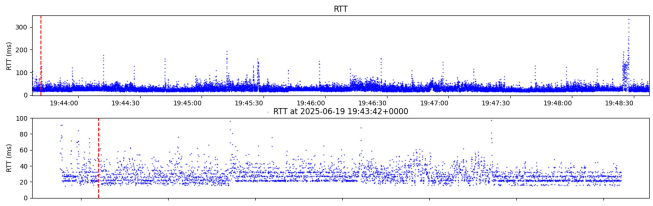

Figure 9. RTT performance during low-speed movement showing communication stability and handover patterns while maintaining slow velocity.

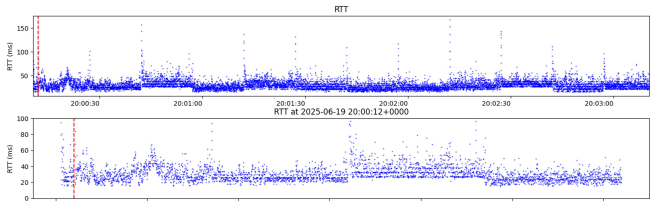

Figure 10. RTT performance during fast-speed movement (2.0 m/s) demonstrating minimal velocity impact on communication quality with slight increase in latency variance.

maintaining consistent environmental conditions while varying movement speed. The robot completed multiple runs at 0.8 m/s (walking speed) and 2.0 m/s (jogging pace), with 5-minute stationary periods between runs for baseline comparison.

Results and Analysis: Figures 9 and 10 show RTT measurements remain remarkably stable at both velocities, concentrated in the 35–45 ms range, with an average of 40.2 ms (± 2.3 ms, 95% CI) at walking speed and 41.8 ms (± 2.7 ms, 95% CI) at jogging speed. The characteristic 15-second satellite handovers appear as step changes regardless of ground velocity. While faster movement introduces marginally higher variance (occasional spikes to 60-70ms vs. consistent 35-45ms at slow speeds), these variations remain within acceptable bounds. This minimal degradation demonstrates Starlink's phased array technology effectively compensates for ground motion through electronic beam steering, contrasting sharply with terrestrial networks where speed typically correlates with degraded performance.

5.2 Impact of Environmental Obstructions

Mobile devices must continuously adapt to changing environmental conditions. Our data captures performance across representative urban environments, demonstrating the profound influence of environmental dynamics on satellite communication.

Open Environment Performance: In unobstructed areas (Figure 11), Starlink exhibits fundamental LEO satellite characteristics. Figure 12 shows periodic RTT fluctuations between 20–40 ms, with a mean of 31.5 ms (± 3.1 ms, 95% CI) in open areas. In contrast, under tree-covered paths (Figure 15), RTT exhibits frequent spikes reaching 40–100 ms, with a mean of 56.4 ms (± 6.2 ms, 95% CI). These patterns remain highly regular, providing a performance baseline for mobile applications.

Figure 11. Environmental context and the robot running scenario in open area showing robot deployment location, surrounding infrastructure, and clear sky conditions from multiple viewpoints.

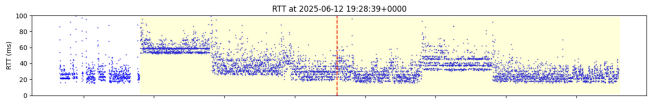

Figure 12. Extended RTT measurements in open environment demonstrating periodic satellite handover patterns and baseline performance characteristics without environmental obstructions.

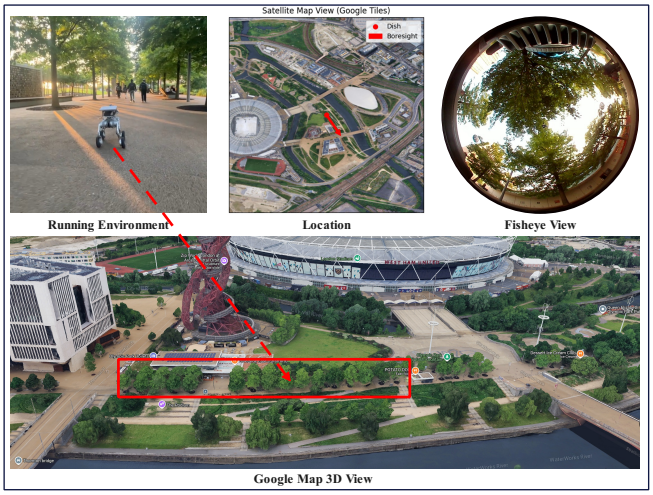

Figure 13. Environmental context and the robot running scenario in tree-covered area showing robot navigation through foliage-dense paths with limited sky visibility.

Obstructed Environment Challenges: Tree-lined streets (Figure 13) create dramatically different conditions. The LiDAR visualization (Figure 14) reveals how dense canopy limits sky visibility to narrow corridors. This constraint fundamentally alters communication dynamics, as shown in Figure 15: RTT exhibits severe instability with frequent spikes reaching 40-100ms. These degradations result from reduced satellite selection options, intermittent signal fluctuations through canopy gaps, and continuous parameter adjustments by obstruction detection algorithms.

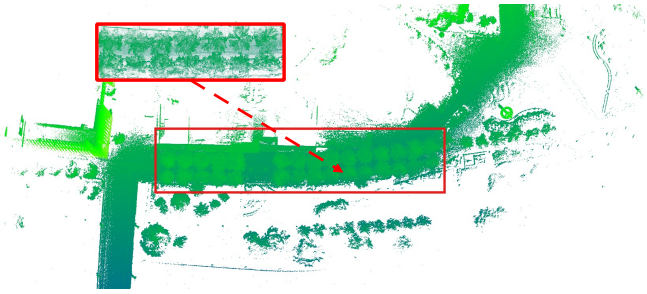

Figure 14. LiDAR point cloud visualization of tree-covered environment illustrating canopy density and potential signal obstruction patterns affecting satellite communication.

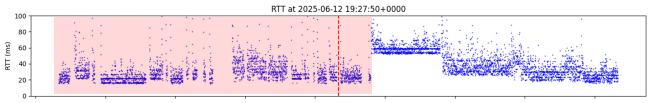

Figure 15. Communication performance in tree-covered environment demonstrating increased RTT instability and frequent spikes due to limited satellite visibility.

Environmental Transitions: The most revealing insights emerge during transitions. When moving from tree cover to open areas, RTT stabilizes within seconds with baseline shifts of 10-20ms and variance reductions exceeding 50%. Unlike terrestrial networks that benefit from multipath propagation, satellite links exhibit binary behavior: sufficient sky visibility enables stable connection, while obstructions cause severe degradation. This distinction makes path planning crucial for mobile satellite applications, as even brief passages under obstructions can disrupt service entirely.

6 Research Opportunities and Conclusion

Our deployable platform and synchronized multi-modal dataset support several concrete research directions in mobile sensing and networked systems. **First, motion-aware networking:** millisecond-aligned RTT measurements with SLAM-derived motion traces can be used to analyze how velocity, acceleration, and orientation correlate with link quality, and to evaluate adaptive transport and scheduling under mobility. **Second, connectivity-aware navigation:** LiDAR geometry and fisheye sky-visibility enable path planning that balances travel distance with expected link continuity, which is relevant to robots and vehicles operating beyond reliable terrestrial coverage. **Third, handover analysis and prediction:** per-satellite azimuth/elevation and connection status provide inputs for modeling handover timing and selection under motion. **Finally, environment-aware adaptation:** point clouds and images capturing canopy density and urban morphology allow policies that adjust bitrate, redundancy, or probing during occlusions.

Our platform and dataset address this research gap by providing synchronized, multi-modal data to correlate communication metrics with motion and environmental context. Open-sourcing these resources provides ground truth for developing adaptive protocols and supports community efforts toward seamless network integration.

References

[1] 2025. CRAWDAD: Community Resource for Archiving Wireless Data at Dartmouth. https://ieee-dataport.org/collections/crawdad. Accessed: 2025-06-18.

[2] 2025. Starlink Business | Maritime. https://www.starlink.com/business/maritime. Accessed: 2025-06-18.

[3] Ali Ahangarpour, Jinwei Zhao, and Jianping Pan. 2024. Trajectory-based Serving Satellite Identification with User Terminal's Field-of-View. In *Proceedings of the 2nd International Workshop on LEO Networking and Communication*. 55–60.

[4] Hayder Al-Hraishawi, Houcine Chougrani, Steven Kisseleff, Eva Lagunas, and Symeon Chatzinotas. 2023. A Survey on Nongeostationary Satellite Systems: The Communication Perspective. *IEEE Communications Surveys Tutorials* 25, 1 (2023), 101–132. doi:10.1109/COMST.2022.3197695

[5] Artie Beaty. 2024. *Google Pixel 9 is first Android phone to get satellite SOS messaging*. https://www.zdnet.com/article/google-pixel-9-is-first-android-phone-to-get-satellite-sos-messaging/

[6] Yan Chen, Xin Ma, and Chaonan Wu. 2024. The concept, technical architecture, applications and impacts of satellite internet: A systematic literature review. *Heliyon* 10, 6 (2024), e33793. doi:10.1016/j.heliyon.2024.e33793

[7] Xia Deng, Le Chang, Shouyuan Zeng, Lin Cai, and Jianping Pan. 2022. Distance-based back-pressure routing for load-balancing LEO satellite networks. *IEEE Transactions on Vehicular Technology* 72, 1 (2022), 1240–1253.

[8] B. Gavish. 1997. Low earth orbit satellite based communication systems — Research opportunities. *European Journal of Operational Research* 99, 2 (1997), 166–179. doi:10.1016/S0377-2217(96)00390-6

[9] Junhao Hu, Lin Cai, Chengcheng Zhao, and Jianping Pan. 2020. Directed percolation routing for ultra-reliable and low-latency services in low earth orbit (LEO) satellite networks. In *2020 IEEE 92nd vehicular technology conference (VTC2020-Fall)*. IEEE, 1–6.

[10] International Telecommunication Union - Radiocommunication Sector (ITU-R). 2021. *Recommendation ITU-R M.2150: Detailed specifications of the radio interfaces of IMT-2020*. Recommendation M.2150-0. International Telecommunication Union. https://www.itu.int/rec/R-REC-M.2150 [accessed 2025-06-18].

[11] Victor Kamel, Jinwei Zhao, Daoping Li, and Jianping Pan. 2024. StarQUIC: Tuning Congestion Control Algorithms for QUIC over LEO Satellite Networks. In *Proceedings of the 2nd International Workshop on LEO Networking and Communication*. 43–48.

[12] Mohamed M Kassem, Aravindh Raman, Diego Perino, and Nishanth Sastry. 2022. A browser-side view of starlink connectivity. In *Proceedings of the 22nd ACM Internet Measurement Conference*. 151–158.

[13] Dominic Laniewski, Eric Lanfer, and Nils Aschenbruck. 2025. Measuring Mobile Starlink Performance: A Comprehensive Look. *IEEE Open Journal of the Communications Society* (2025).

[14] Daoping Li, Jinwei Zhao, and Jianping Pan. 2025. FTRL-WRR: Learning-Based Two-Path Scheduler for LEO Networks. In *2025 IEEE 22nd Consumer Communications & Networking Conference (CCNC)*. IEEE, 1–6.

[15] Tengfei Liu, Tingting Wang, Ye Li, Jinwei Zhao, Ruifeng Gao, and Jianping Pan. 2025. Modeling Packet Loss of Low-Earth Orbit Satellite Networks. In *2025 IEEE Wireless Communications and Networking Conference (WCNC)*. IEEE, 1–6.

[16] Ivan Mehta. 2023. *Samsung unveils its own solution for satellite-based smartphone communication*. https://techcrunch.com/2023/02/23/samsung-unveils-its-own-solution-for-satellite-based-smartphone-communication/

[17] Jianping Pan, Jinwei Zhao, and Lin Cai. 2023. Measuring a low-earth-orbit satellite network. In *2023 IEEE 34th Annual International Symposium on Personal, Indoor and Mobile Radio Communications (PIMRC)*. IEEE, 1–6.

[18] Jianping Pan, Jinwei Zhao, and Lin Cai. 2024. Measuring the satellite links of a LEO network. In *ICC 2024-IEEE International Conference on Communications*. IEEE, 4439–4444.

[19] Valentin Platzgummer, Vaclav Raida, Gerfried Krainz, Philipp Svoboda, Martin Lerch, and Markus Rupp. 2019. UAV-based coverage measurement method for 5G. In *2019 IEEE 90th Vehicular Technology Conference (VTC2019-Fall)*. IEEE, 1–6.

[20] Weibiao Tian, Ye Li, Jinwei Zhao, Sheng Wu, and Jianping Pan. 2024. An eBPF-Based Trace-Driven Emulation Method for Satellite Networks. *IEEE Networking Letters* (2024).

[21] Muhammad Asad Ullah, Antti Heikkinen, Mikko Uitto, Antti Anttonen, and Konstantin Mikhaylov. 2025. Impact of Weather on Satellite Communication: Evaluating Starlink Resilience. *arXiv preprint arXiv:2505.04772* (2025).

[22] Mojtaba Vaezi, Amin Azari, Saeed R. Khosravirad, Mahyar Shirvanimoghaddam, M. Mahdi Azari, Danai Chasaki, and Petar Popovski. 2022. Cellular, Wide-Area, and Non-Terrestrial IoT: A Survey on 5G Advances and the Road Toward 6G. *IEEE Communications Surveys Tutorials* 24, 2 (2022), 1117–1174. doi:10.1109/COMST.2022.3151028

[23] Bingsen Wang, Xiaohui Zhang, Shuai Wang, Li Chen, Jinwei Zhao, Jianping Pan, Dan Li, and Yong Jiang. 2024. A Large-Scale IPv6-Based Measurement of the Starlink Network. *arXiv preprint arXiv:2412.18243* (2024).

[24] Yufei Wang, Lin Cai, and Jun Liu. 2023. High-Reliability, Low-Latency, and Load-Balancing Multipath Routing for LEO Satellite Networks. In *2023 Biennial Symposium on Communications (BSC)*. IEEE, 107–111.

[25] Wikipedia. [n. d.]. *Starlink*. https://en.wikipedia.org/wiki/Starlink

[26] Wenjun Yang, Lin Cai, Shengjie Shu, and Jianping Pan. 2024. Mobility-aware congestion control for multipath QUIC in integrated terrestrial satellite networks. *IEEE Transactions on Mobile Computing* (2024).

[27] Wenjun Yang, Shengjie Shu, Lin Cai, and Jianping Pan. 2021. MM-QUIC: Mobility-aware multipath QUIC for satellite networks. In *2021 17th International Conference on Mobility, Sensing and Networking (MSN)*. IEEE, 608–615.

[28] Jinwei Zhao and Jianping Pan. 2024. LENS: A LEO Satellite Network Measurement Dataset. In *Proceedings of the 15th ACM Multimedia Systems Conference*. 278–284.

[29] Jinwei Zhao and Jianping Pan. 2024. Low-Latency Live Video Streaming over a Low-Earth-Orbit Satellite Network with DASH. In *Proceedings of the 15th ACM Multimedia Systems Conference*. 109–120.

[30] Jinwei Zhao and Jianping Pan. 2025. LEOViz: Real-time Visualization of LEO Satellite Networks. https://github.com/clarkzjw/LEOViz. (2025).

[31] Jinkai Zheng, Tom H Luan, Guanjie Li, Yanfeng Zhang, Mingfeng Yuan, and Jianping Pan. 2025. QTER: QoS-Aware Three-Dimensional Efficient and Reliable Routing for LEO Satellite Networks. *IEEE Internet of Things Journal* (2025).

[32] Jinkai Zheng, Tom H Luan, Jinwei Zhao, Guanjie Li, Yao Zhang, Jianping Pan, and Nan Cheng. 2024. Adaptive Multi-Link Data Allocation for LEO Satellite Networks. In *GLOBECOM 2024-2024 IEEE Global Communications Conference*. IEEE, 3021–3026.